Application of a PC-Controlled MW-Spectrometer for the Analysis of Ketene-D_2. Simultaneous Analysis of Vibrational Excited States Using Microwave and Infrared Spectra

J. Doose, A. Guarnieri, W. Neustock, R. Schwarz, F. Winther
Institute for Physical Chemistry, University of Kiel, Kiel, F.R. Germany

F. Hegelund
Department of Chemistry, Aarhus University, DK-8000 Aarhus C, Denmark

Z. Naturforsch. **44a**, 538–550 (1989); received March 17, 1989

D_2CCO has been investigated in the first excited vibrational states of the ν_9, ν_6, and ν_5 vibrations. About 150 transitions have been measured partly at room temperature and partly at 360 K using a micro- and millimeter-wave spectrometer provided with an averaging system using a personal computer. Rotational and centrifugal distortion constants have been obtained for the excited states mentioned. A simultaneous least squares analysis of these MW-data with upper state combination differences obtained from FT-IR data has been carried out. Improved sets of molecular parameters have been obtained.

I. Introduction

Ketene was the subject of some of the earliest microwave studies because of its relatively simple structure and its importance for chemical synthesis [1–3].

The microwave and infrared studies of the HD and D_2 substituted species [2–5] gave information about the molecular geometry.

Nemes and Winnewisser [6] measured a-type rotational transitions of the ground state of Ketene-d_1, and Ketene-d_2, in the frequency range from 8 GHz to 220 GHz, and analysed the spectrum in terms of Watson's a-reduced Hamiltonian, including the sextic terms H_{KJ} and H_{JK}. In addition they determined values of the inertial defect and the τ defects [6]. During these measurements they observed and measured also some lines belonging to vibrationally excited states, but did not analyze them [7].

The in-plane vibration ν_9 (371.6 cm^{-1}), belonging to the B_2 species and the out of-plane vibrations ν_6 (434.7 cm^{-1}) and ν_5 (541.2 cm^{-1}), belonging to the B_1 species, correspond to the lowest vibrational levels of D_2C_2O and are appreciably populated at temperatures from 300 to 360 K. Recently Hegelund et al. [8] investigated the high resolution IR-spectrum of D_2C_2O and published the constants for the excited vibrational states ν_9, ν_6, and ν_5. Since no microwave work exists concerning the excited states and possible shifts of the rotational lines due to Coriolis interaction, we started an investigation of these three excited vibrational states with the purpose of considering the problem from the pure rotational point of view.

Reprint requests to Prof. Dr. A. Guarnieri, Institut für Physikalische Chemie, Universität Kiel, Olshausenstr. 40, D-2300 Kiel 1.

II. Experimental Details

The IR measurements were carried out with the Fourier Transform spectrometer at the University of Oulu [9, 10] and have been described in [8].

The measurements in the microwave region have been made at the University of Kiel, using an averaging technique with an IBM-AT-Clone (PC), as described below. A block diagram of the experimental arrangement is shown in Figure 1. The spectrometer was mainly used in the source modulation mode.

1. Frequency Control

The standard frequency is provided by a frequency synthesizer PTS 500 (TEXCAN), whose standard is a 10 MHz-signal derived from the 77.5 kHz signal of the broadcasting station DCF 77 (Mainflingen, Germany). A 77.5 kHz receiver XKE2 (ROHDE & SCHWARZ) is combined with a crystal oscillator

0932-0784 / 89 / 0600-0538 $ 01.30/0. – Please order a reprint rather than making your own copy.

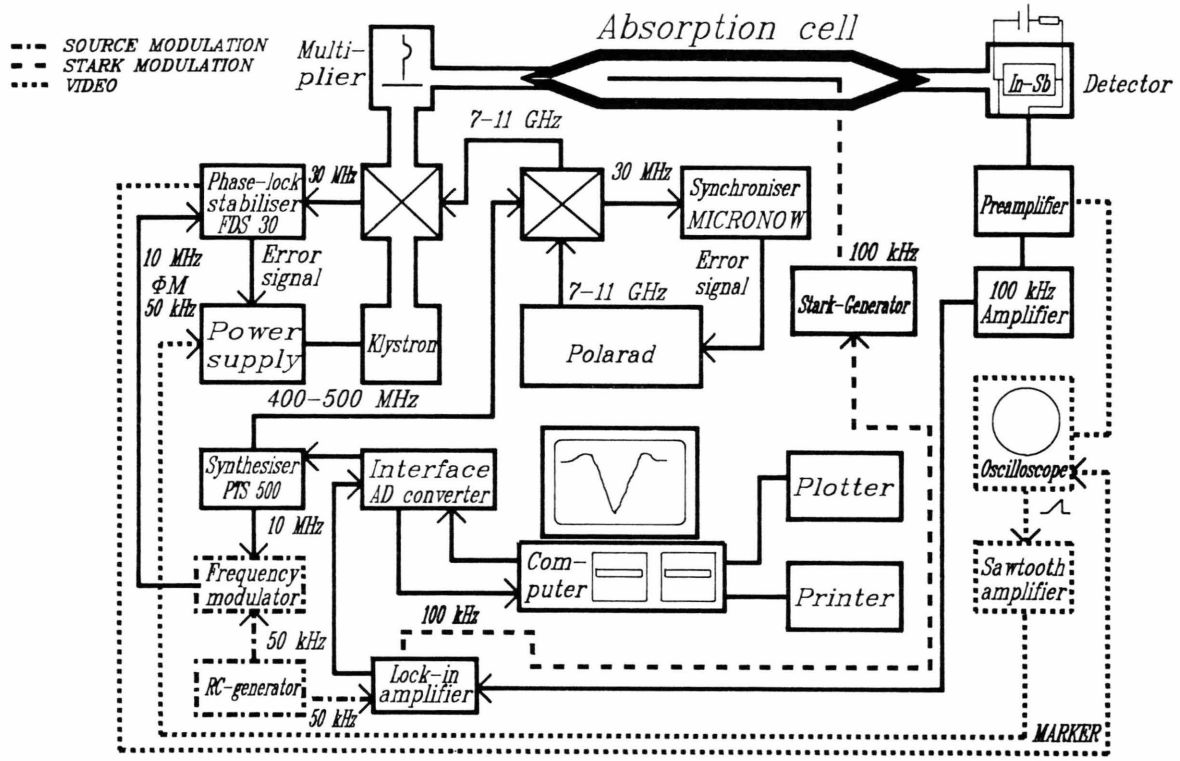

Fig. 1. Experimental setup.

XSD2 (ROHDE & SCHWARZ) to yield a 5 MHz signal with a relative accuracy of 5×10^{-10}. This signal is used to drive the synthesizer after multiplication by two.

The output-frequency of the PTS 500 has been used for the stabilisation of the klystrons through two loops in the usual way.

2. *Interface*

The PTS Synthesizer is driven by means of a PC in the following way (see Figure 2):

2.1 Output to PTS500

The core of the driver is a set of 10 BCD-counters 74LS192. The outputs $Q_1 \ldots Q_4$ are connected to the inputs of 10 BCD-to-7-segment decoders 74LS47 and further via inverters 74LS04 to the corresponding inputs of the PTS500. The 74LS47 drive 7-segment displays HA1181r.

2.2 Setting of Counters

If the input 'Load' (Pin 11) of the BCD-counter is set to zero, the counter enters the desired data at inputs $D_0 \ldots D_3$ (Pin 15, 1, 10, 9). To load the 10 counters separately we chose a NAND-gate:

Table 1. NAND-gate.

A	*B*	*Y*
0	0	1
0	1	1
1	0	1
1	1	0

The *A* input of the gate was connected with the command 'Load' coming from the PC. The *B* input was connected to the inverting output of one of the 74LS47's. With these decoders it is possible to choose (via LSELECT A ... D) the counter, to which the arriving data (LOAD A ... D) have to be read in. This is controlled by the computer. If the LOAD-signal and the corresponding decoder output are high, the input of the counter is low (Table 2) and the data are accepted.

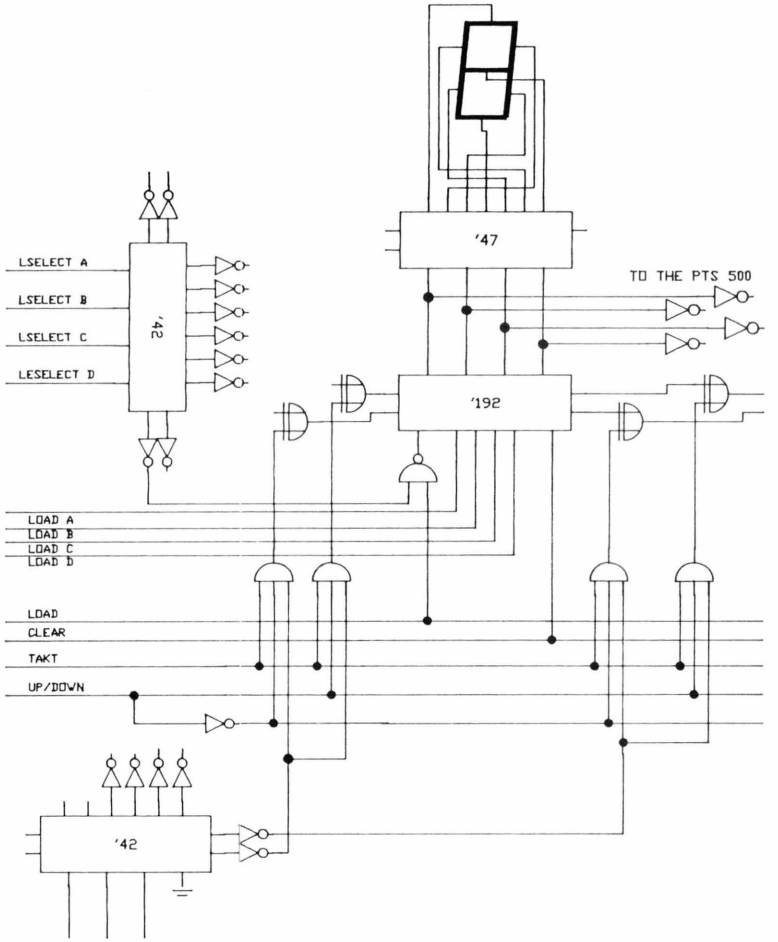

Fig. 2. Schema of the PTS 500 controlling system.

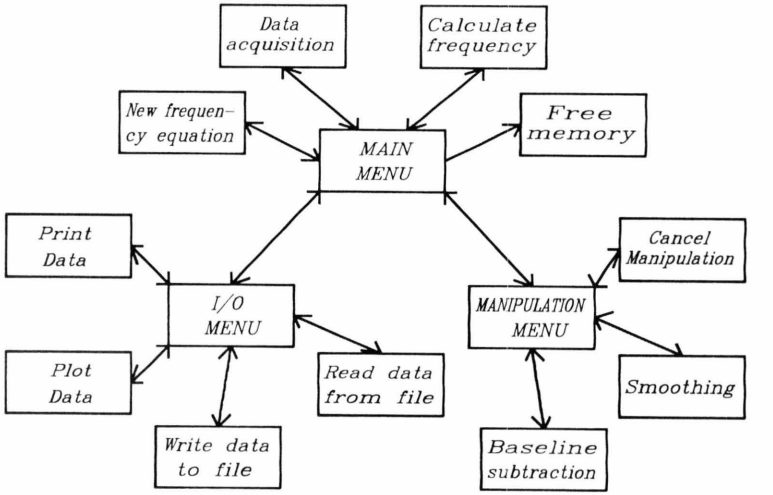

Fig. 3. Program structure

Table 4. Technical details of the data acquisition system.

Computer	IBM Clone, 80286, 10 MHz Hercules Graphic Card
A/D Converter	8 Bit
PTS 500	1 Hz to 499.9999998 MHz Parallel-entry, BCD-code
Switching time	20 µs
Number of points	2048 (up and down sweep)
max. repetition rate with display and scaling	10240 points/s 100 µs/point
without display and scaling	50 µs/point
max. number of cycles	32767
Display	horizontal 512 points vertical 256 points (up sweep only)
Software	written in Pascal

2.3 Supply of Clock

Our system is able to sweep in steps from 0.1 Hz to 10 kHz. We did not use the usual way, i.e. that of connecting the outputs CARRY and BORROW of the lower frequency digit directly to the inputs UP and DOWN of the higher digit. We inserted instead an XOR-gate (74LS86) between them with the CARRY/BORROW signal at one input and clock signal at the other. Thus we are able to direct the clock signal to every counter we choose.

Table 2. XOR-gate.

A	*B*	*Y*
0	0	0
0	1	1
1	0	1
1	1	0

The A input of the gate is connected to the CARRY respectively BORROW-output of the counter (in rest position "high"). The B input of the XOR-gate connects the output of a 3I-AND-gate (74LS11).

Table 3. 3I-AND-gate.

A	*B*	*C*	*Y*
0	0	0	0
0	0	1	0
0	1	0	0
0	1	1	0
1	0	0	0
1	0	1	0
1	1	0	0
1	1	1	1

The following three signals are at the inputs of this gate:

A: An inverted signal from the Decoder (74LS42) to choose the frequency digit.
B: A signal to indicate the direction of counting.
C: The clock.

If the first two signals are "high", the clock can switch the output of the 3I-AND-gate (Table 3).

2.4 Detector Signal Conversion

On the detector side, the signal was processed by an 8-Bit-AD converter AD570, protected by a 15 Ohm resistor. We clipped voltages greater than 5 V with 2 Z-diodes. The last step is the handing over of the digital signals to the PC with the help of a power inverter 74AS1004.

2.5 Sweep Procedure

The frequency sweep was performed by switching 1024 frequency steps for up-sweep and 1024 frequency steps for down-sweep. The frequency steps are produced by reading the start frequency into the cascaded BCD-counters and then stepping one of them. The computer calculates the start frequency, the digit of the BCD-counter which has to be switched, and stores the corresponding value coming from the AD-converter. After each up- and down-cycle the up-sweep is displayed on the monitor. This procedure is very fast, and it is possible to repeat the whole cycle with a repetition frequency of 5 Hz. The technical details are given in Table 4.

2.6 Software

After the data acquisition has been completed, the program, written in Pascal, allows a lot of manipulations of the data set as shown in Figure 3.

Three menus help the user to handle the program.

The main menu has the option of calling the input/output- and manipulation-submenu. During recording of the data the normalized averaged upsweep is presented on the monitor.

To determine the frequency of maximum absorption, a Lorentzian-lineshape is fitted to the experimental data up to half maximum intensity.

The I/O menu allows storage, reading, printing and plotting of data. The manipulation menu handles operations like smoothing (according to Savitzky and Golay [11]) and mode suppression.

An example of lines of ketene-d_2 in the range 53068.6 MHz to 53079.842 MHz is given in Figure 4. In addition two kinds of manipulations are shown, namely mode subtraction and smoothing.

3. Detection

Detection of the microwaves has been done with an InSb bolometer in the usual way [13].

4. Phasemodulator

There are two demands concerning the modulation: First, the MW-source has to be swept phase locked to ensure a satisfactory frequency accuracy, and, second, a higher sensitivity should be achieved by using source (frequency) modulation. For this purpose a frequency

Fig. 4a. Acquired data of a survey of the microwave spectrum of D_2-ketene from 53068.6 MHz to 53079.842 MHz.

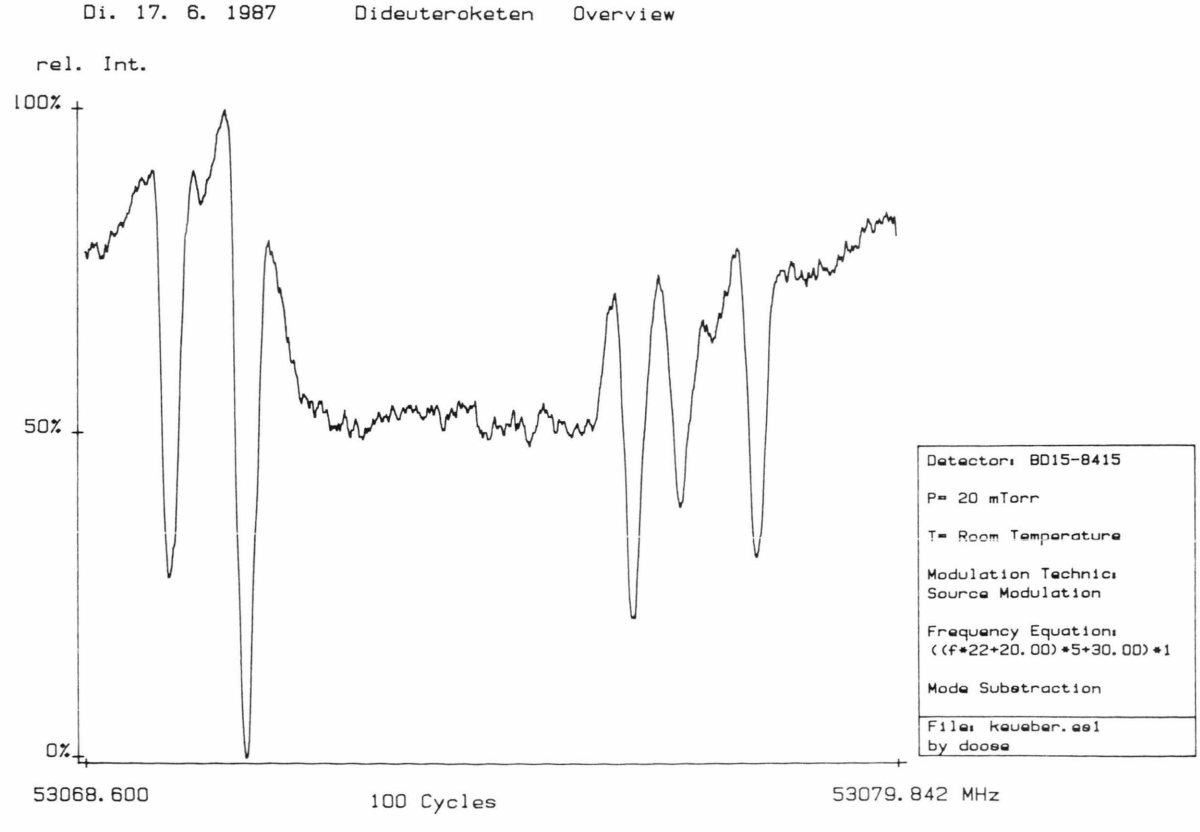

Fig. 4b. Data of Fig. 4a after mode subtraction.

Fig. 4c. Data of Fig. 4a after mode subtraction and smoothing procedure.

modulated signal is fed into the reference input of the synchronizer in the stabilisation loop.

In the case of the FDS30-stabilizer we use a modulated 10 MHz signal. As we wish to utilize fully the accuracy offered by the frequency standard, the frequency modulated carrier frequency has to retain its absolute precision. Thus we use a phase modulation technique. Since the modulation frequency f_{mod} is constant, the phase modulation is equivalent to a frequency modulation.

To estimate the required phase deviation we look at the modulation and detection system used.

In the case of an absorption line a frequency modulation of the source produces an amplitude modulation of the detected microwave power. Subsequent demodulation yields the molecular absorption signal. In our set up we use a lock-in amplifier (Ithaco 393) working in the 2 f-mode.

To guarantee a sufficient level of the 2 f-amplitude-signal at the maximum of the absorption line the frequency deviation of a frequency modulated MW-source has to be of the same order of magnitude as the line width.

On the other hand this frequency deviation is limited by the condition of having no 2 f-signal in the quasilinear part of an absorption line, which is represented by its slope. A deviation of the half width of the absorption line satisfies both conditions. Assuming a line width in the MMW-range of 0.5 MHz, the corresponding frequency deviation of the MW-frequency, as well as of the 30 MHz synchronizer working frequency, is about 0.25 MHz.

The synchronizer (Schomandl FDS30) operates with an external reference frequency of 10 MHz, which is multiplied internally to the working frequency of 30 MHz. Thus we need a frequency deviation ΔF of $\Delta F = 0.25/3$ MHz $= 83$ kHz for the 10 MHz reference.

Having a modulation frequency f_{mod} of 16 kHz, the resulting phase shift is

$$\Delta\Phi = \frac{\Delta F}{f_{\text{mod}}} = \frac{83\ \text{kHz}}{16\ \text{kHz}} = 5.2\ \text{rad} = 300^\circ\,.$$

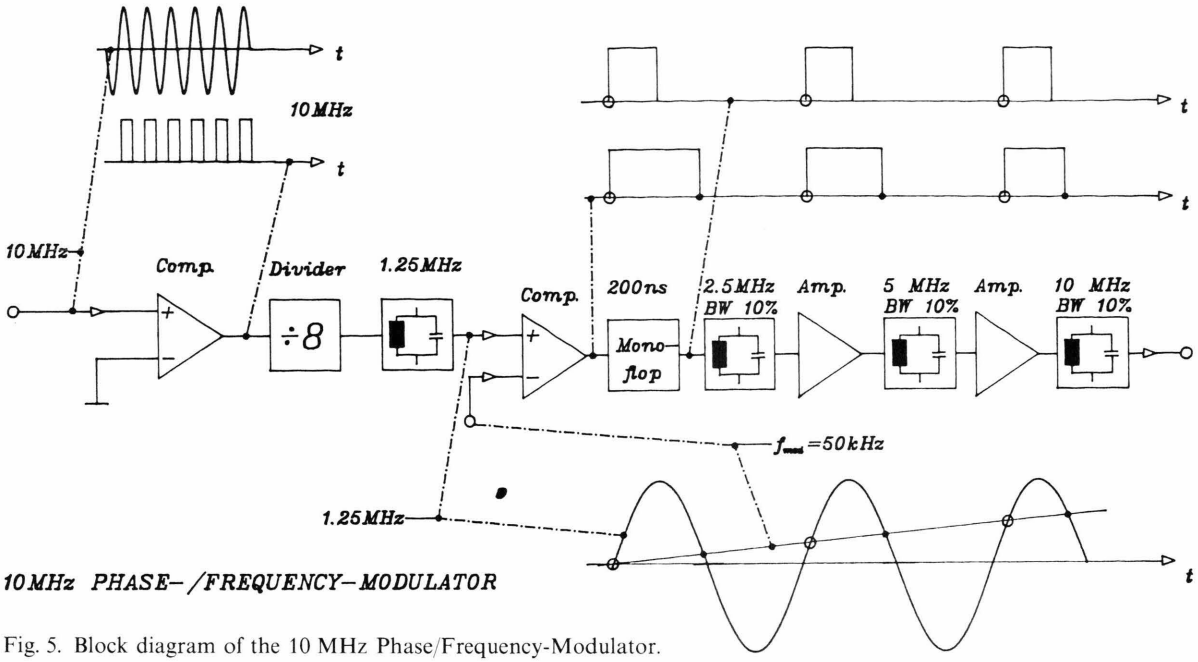

Fig. 5. Block diagram of the 10 MHz Phase/Frequency-Modulator.

A modulation frequency of 50 kHz would require a phase shift of only 100°.

It is only possible to get phase shifts of this magnitude by using frequency multiplication. The multiplication factor for the frequency is the same as for the phase shift.

In our phase modulator (Fig. 5) we use electronic circuits which allow maximum phase shifts of 45°, and therefore we need frequency multiplication greater than $300°/45° = 6.7$.

Thus a factor of eight would solve the problem. Consequently in a first step we divide the 10 MHz reference by eight to get a frequency of 1.25 MHz. The second step is the phase modulation up to 45° followed by a frequency multiplication, again by a factor of eight.

The resulting maximum phase shift is in the order of magnitude of $8 \times 45° = 360°$.

The phase modulation of the 1.25 MHz sinewave is done by a comparator (AM686DC), whose working principle is to compare the continuous 1.25 MHz input voltage with the modulation voltage as a reference voltage. When the voltage of the 1.25 MHz signal is larger than the reference level, the comparator output delivers a square wave voltage (Figure 5).

The interesting part of the resulting square wave is the ascending slope, which is determined by the points (circles in Fig. 5) when the 1.25 MHz input voltage exceeds the reference voltage.

Since the comparator reference voltage varies with the level of the modulation voltage, the ascending slope of the output square wave shifts simultaneously.

If care is taken that the adjustable amplitude of the modulation voltage is limited to 70% of the amplitude of the 1.25 MHz signal, the resulting phase shift of the square wave will deviate less than ten per cent from linearity.

The maximum length of the square wave pulses at the comparator output is not constant. To obtain a constant output amplitude from the following frequency multiplier, a constant maximum length of the square wave is necessary. To achieve this, the output voltage of the comparator is applied to a monoflop (74LS121). The pulse length is fitted to the resonance frequency of the following 2.5 MHz doubling circuit (200 ns).

Two further doubling circuits produce the desired output frequency of 10 MHz.

5. *Synthesis of D_2C_2O*

The deuteroketene sample was synthesized by gas phase pyrolysis of perdeutero-acetone with a ketene-lamp as described in [12]. The major impuri-

Table 5. Rotational transition frequencies (MHz) of ketene-d_2 in the $v_5 = 1$ state. Measured frequencies were obtained with our computer controlled spectrometer; the calculated frequencies were obtained with the *s*-reduced constants from the MW fit. – The last figure has poor significance. Transitions with ** have been measured by Nemes and Winnewisser [7]. Transitions with * are given in [2, 3, 14].

J'	K'_-	K'_+	J	K_-	K_+	obs. [MHz]	calc. [MHz]	obs–calc [kHz]
1	0	1	0	0	0	17695.000*	17694.957	43
2	0	2	1	0	1	35388.200*	35388.154	46
2	1	1	1	1	0	35941.430*	35941.541	-111
2	1	2	1	1	1	34835.370*	34835.562	-192
3	0	3	2	0	2	53077.855	53077.829	26
3	1	2	2	1	1	53911.099	53911.084	15
3	1	3	2	1	2	52252.130	52252.145	- 15
3	2	1	2	2	0	53083.583	53083.585	- 2
3	2	2	2	2	1	53076.814	53076.803	11
4	0	4	3	0	3	70762.146	70762.224	- 78
4	1	4	3	1	3	69667.386	69667.294	92
4	1	3	3	1	2	71879.233	71879.150	83
4	2	3	3	2	2	70767.621	70767.481	140
4	2	2	3	2	1	70784.302	70784.435	-132
4	3	2	3	3	1	70758.939	70758.996	- 57
4	3	1	3	3	0		70759.015	- 76
5	0	5	4	0	4	88439.589	88439.579	10
5	1	5	4	1	4	87080.568	87080.539	29
5	1	4	4	1	3	89845.268	89845.239	29
5	2	3	4	2	2	88490.820	88490.700	120
5	2	4	4	2	3	88456.765	88456.795	- 30
5	3	2	4	3	1	88449.780	88449.938	-158
5	4	1	4	4	0	88424.704	88424.530	174
5	4	2	4	4	1		88424.530	174
5	3	3	4	3	2	88449.780	88449.871	- 90
6	0	6	5	0	5	106108.107	106108.141	- 34
6	1	5	5	1	4	107808.825	107808.844	- 20
6	1	6	5	1	5	104491.446	104491.417	29
6	2	5	5	2	4	106144.515	106144.407	109
6	2	4	5	2	3	106203.644	106203.730	- 86
6	3	3	5	3	2	106141.577	106141.659	- 82
6	3	4	5	3	3		106141.478	99
6	5	1	5	5	0	106071.966	106072.016	- 50
6	5	2	5	5	1		106072.016	- 50
7	1	7	6	1	6	121899.471	121899.471	0
8	1	8	7	1	7	139304.267**	139304.255	11
8	1	7	7	1	6	143726.530**	143726.536	- 6
8	2	6	7	2	5	141655.450**	141655.435	15
8	2	7	7	2	6	141513.138**	141513.157	- 18
8	3	5	7	3	4	141528.184**	141528.211	- 27
8	3	6	7	3	5	141527.359**	141527.397	- 38
8	4	4	7	4	3	141482.050**	141482.065	- 16
8	4	5	7	4	4		141482.064	- 14
9	0	9	8	0	8	159043.654**	159043.663	- 9
9	1	8	8	1	7	161679.595**	161679.563	32
9	1	9	8	1	8	156705.342**	156705.335	7
9	2	7	8	2	6	159396.766**	159396.749	17
9	2	8	8	2	7	159193.598**	159193.614	- 17
9	3	6	8	3	5	159223.387**	159223.428	- 42
9	3	7	8	3	6	159221.909**	159221.936	- 27
9	4	5	8	4	4	159168.750**	159168.706	43
9	4	6	8	4	5		159168.702	47

Table 6. Rotational transition frequencies (MHz) of ketene-d_2 in the $v_6 = 1$ state. Measured frequencies were obtained with our computer controlled spectrometer; the calculated frequencies were obtained with the *s*-reduced constants from the MW fit. – The last figure has poor significance. – Transitions with ** have been measured by Nemes and Winnewisser [7]. Transitions with * are given in references [2, 3, 14].

J'	K'_-	K'_+	J	K_-	K_+	obs. [MHz]	calc. [MHz]	obs–calc [kHz]
1	0	1	0	0	0	17692.590*	17692.492	98
2	0	2	1	0	1	35383.360*	35383.312	48
2	1	1	1	1	0	35924.400*	35924.361	39
2	1	2	1	1	1	34842.900*	34842.954	- 54
3	0	3	2	0	2	53070.758	53070.788	- 30
3	1	2	2	1	1	53885.385	53885.370	15
3	1	3	2	1	2	52263.304	52263.288	16
3	2	1	2	2	0	53076.163	53076.084	79
3	2	2	2	2	1	53069.710	53069.646	64
4	0	4	3	0	3	70753.178	70753.247	- 69
4	1	3	3	1	2	71845.048	71844.969	79
4	1	4	3	1	3	69682.316	69682.252	64
4	2	3	3	2	2	70758.157	70758.059	98
4	3	1	3	3	0	70749.925	70749.845	80
4	3	2	3	3	1		70749.827	98
4	2	2	3	2	1	70774.096	70774.153	- 57
5	0	5	4	0	4	88428.966	88429.020	- 53
5	1	4	4	1	3	89802.697	89802.682	16
5	1	5	4	1	4	87099.367	87099.399	- 32
5	2	3	4	2	2	88477.416	88477.398	18
5	2	4	4	2	3	88445.205	88445.213	- 8
5	3	2	4	3	1	88438.539	88438.704	-164
5	3	3	4	3	2		88438.640	-101
5	4	1	4	4	0	88414.220	88414.207	13
5	4	2	4	4	1		88414.207	13
6	1	5	5	1	4	107757.983	107758.025	- 43
6	1	6	5	1	5	104514.318	104514.286	32
6	2	4	5	2	3	106187.039	106187.108	- 69
6	2	5	5	2	4	106130.691	106130.794	-103
6	3	3	5	3	2	106128.490	106128.511	- 21
6	3	4	5	3	3		106128.343	148
6	5	1	5	5	0	106061.627	106061.660	- 33
6	5	2	5	5	1		106061.660	- 33
7	1	7	6	1	6	121926.450	121926.476	- 26
7	5	2	6	5	1	123740.746	123740.720	26
7	5	3	6	5	2		123740.720	26
8	1	7	7	1	6	143659.627**	143659.632	- 5
8	1	8	7	1	7	139335.575**	139335.543	32
8	3	5	7	3	4	141511.805**	141511.806	- 1
8	3	6	7	3	5	141511.029**	141511.047	- 18
9	1	8	8	1	7	161604.890**	161604.886	4
9	1	9	8	1	8	156741.088**	156741.071	17
9	3	6	8	3	5	159205.729**	159205.734	- 5
9	3	7	8	3	6	159204.342**	159204.343	- 1
10	0	10	9	0	9	176649.574	176649.586	- 13
12	1	11	11	1	10	215412.155	215412.138	17

Table 7. Rotational transition frequencies (MHz) of ketene-d_2 in the $v_9 = 1$ state. Measured frequencies were obtained with our computer controlled spectrometer; the calculated frequencies were obtained with the *s*-reduced constants from the MW fit. – The last figure has poor significance. Transitions with ** have been measured by Nemes and Winnewisser [7]. Transitions with * are given in references [2, 3, 14].

J'	K'_-	K'_+	J	K_-	K_+	obs. [MHz]	calc. [MHz]	obs calc [kHz]
1	0	1	0	0	0	17727.130*	17727.037	93
2	0	2	1	0	1	35451.850*	35451.837	13
2	1	1	1	1	0	36048.800*	36048.818	18
2	1	2	1	1	1	34857.040*	34856.941	99
3	0	3	2	0	2	53172.149	53172.161	- 12
3	1	2	2	1	1	54071.678	54071.686	- 8
3	1	3	2	1	2	52283.863	52283.904	- 41
3	2	1	2	2	0	53182.657	53182.699	- 42
3	2	2	2	2	1	53173.978	53174.004	- 26
4	1	4	3	1	3	69709.054	69709.067	- 13
4	0	4	3	0	3	70885.810	70885.774	36
4	2	3	3	2	2	70896.856	70896.677	179
4	1	3	3	1	2	72092.617	72092.699	- 81
5	0	5	4	0	4	88590.604	88590.442	162
5	1	4	4	1	3	90111.222	90111.225	- 4
5	1	5	4	1	4	87131.771	87131.840	- 69
5	2	4	4	2	3	88617.694	88617.639	55
5	2	3	4	2	2	88660.955	88661.105	-151
5	3	2	4	3	1	88615.480	88615.389	91
5	3	3	4	3	2		88615.284	196
6	0	6	5	0	5	106283.839	106283.939	-100
6	1	5	5	1	4	108126.581	108126.625	- 45
6	1	6	5	1	5	104551.547	104551.643	- 96
6	2	4	5	2	3	106412.366	106412.511	-145
6	2	5	5	2	4	106336.443	106336.463	- 19
6	3	3	5	3	2	106340.964	106340.884	80
6	5	1	5	5	0	106273.943	106274.007	- 64
6	5	2	5	5	1		106274.007	- 64
8	1	7	7	1	6	144145.419**	144145.421	- 2
8	1	8	7	1	7	139380.100**	139380.094	5
8	2	7	7	2	6	141765.947**	141765.988	- 40
8	3	5	7	3	4	141796.318**	141796.230	87
8	3	6	7	3	5	141795.064**	141794.976	88
9	1	8	8	1	7	162147.482**	162147.463	18
9	1	9	8	1	8	156787.692**	156787.655	37
9	2	7	8	2	6	159736.169**	159736.106	62
9	2	8	8	2	7	159475.838**	159475.834	3
9	3	6	8	3	5	159526.543**	159526.630	- 87
9	3	7	8	3	6	159524.272**	159524.331	- 60
9	8	1	8	8	0	159149.372**	159149.367	5
9	8	2	8	8	1		159149.367	5

Table 8. Molecular parameters of D_2C_2O in the $v_5 = 1$ state. * Fixed to the IR-MW value (Table 15). – The correlation coefficients which are near 1 in the *a*-reduced MW fit do not exceed the value of 0.8 in the IR-MW fit.

ROTATIONAL CONSTANTS

	Watson's s-reduced			Watson's a-reduced		
A	145474(59)	MHz		145474(59)	MHz	
B	9116.607(6)	MHz		9116.23(20)	MHz	
C	8575.897(7)	MHz		8576.27(20)	MHz	
D_J	2.80(3)	kHz		Δ_J 2.62(10)	kHz	
D_{JK}	0.3162(6)	MHz		Δ_{JK} 0.3173(8)	MHz	
D_K	2.7131	MHz	*	Δ_K 2.7131	MHz	*
d_1	-0.20(2)	kHz		δ_J 0.20(2)	kHz	
d_2	0.09(5)	kHz		δ_K -0.19(9)	MHz	
H_{JK}	0.234(4)	kHz		Φ_{JK} 0.234(4)	kHz	
H_{KJ}	-0.69(2)	kHz		Φ_{KJ} -0.69(2)	kHz	

κ -.9921

CORRELATION MATRIX

	A	B	C	D_J	D_{JK}	d_1	d_2	H_{JK}	H_{KJ}
A	1.000								
B	-.211	1.000							
C	.318	-.682	1.000						
D_J	.709	-.144	.662	1.000					
D_{JK}	-.139	.273	.259	.273	1.000				
d_1	-.429	-.724	.889	.662	.059	1.000			
d_2	.286	-.134	.144	.188	-.046	.247	1.000		
H_{JK}	.531	-.059	.448	.738	.569	.421	.142	1.000	
H_{KJ}	-.510	.324	-.029	-.216	.765	-.220	-.146	-.050	1.000

	A	B	C	Δ_J	Δ_{JK}	δ_J	δ_K	Φ_{JK}	Φ_{KJ}
A	1.000								
B	-.292	1.000							
C	.297	-1.000	1.000						
Δ_J	-.096	.962	-.956	1.000					
Δ_{JK}	.110	-.694	.706	-.619	1.000				
δ_J	-.429	.269	-.279	-.070	-.224	1.000			
δ_K	-.287	1.000	-.999	.963	-.700	.248	1.000		
Φ_{JK}	.549	-.238	.253	-.037	.570	-.437	-.238	1.000	
Φ_{KJ}	-.525	.231	-.222	.163	.379	.236	.222	-.081	1.000

STANDARD DEVIATION 66 kHz

ties in the preparation were $D_2C=CD_2$, $DC\equiv CD$, $D_3C-CD=CD_2$ and $(D_3C)_2CO$, which could be partially removed by low temperature distillation.

Measurements have been made in a heatable cell made of brass, using sample pressures in the range of 20–40 mTorr (2.7–5.3 Pa).

III. Results

1. Pure Rotation Transitions

The microwave and millimeter wave rotational spectra show the structure expected for *a*-type transitions of a slightly asymmetric prolate top molecule.

Starting values for the prediction of the spectra were low frequency lines measured in [3, 14]. These lines are labelled with (*) in Tables 5, 6, and 7. Lines in the millimeter range were identified partly through the Stark effect and partly by means of double resonance experiments. Subsequently it was possible to identify the lines marked with (**) already measured by Nemes and Winnewisser during their investigation of the ground state [7].

The fit of the measured frequencies has been made using Watson's *s*-reduced Hamiltonian in the I^r axis representation because the molecule is near the prolate symmetric top limit:

$$H_{\text{red}} = A P_a^2 + B P_b^2 + C P_c^2 - D_J (P^2)^2 - D_{JK} P^2 P_a^2 - D_K P_a^4 + d_1 P^2 (P_+^2 + P_-^2) + d_2 (P_+^4 + P_-^4) + H_{JK} (P^2)^2 P_a^2 + H_{KJ} P^2 P_a^4 \; .$$

With the purpose of comparing our data with those obtained by IR-analysis, we also performed a fit using Watson's *a*-reduced Hamiltonian:

$$H_{\text{red}} = A P_a^2 + B P_b^2 + C P_c^2 - \Delta_J (P^2)^2 - \Delta_{JK} P^2 P_a^2 - \Delta_K P_a^4 - 1/2 [\delta_J P^2 + \delta_K P_a^2, P_+^2 + P_-^2]_+ + \Phi_{JK} (P^2)^2 P_a^2 + \Phi_{KJ} P^2 P_a^4 \; .$$

The results of both fits are given in Tables 8, 9, and 10.

As expected, the obtained values of the parameters in the Watson's *a*-reduced fit show a larger error than in the other case. A similar feature can be observed in the correlation matrices, where the correlation coefficients for the *a*-fit are sometimes near the 1 limit.

In order to compare our data with those of the ground state we made a recalculation of the ground state constants (Table 11) using a similar set of lines as for the excited states. The resulting standard deviation is not the same as that given in [6] because of the different number of considered lines; nevertheless it is considerably smaller than in the excited states because of the higher accuracy reached through measurements of stronger ground state lines.

2. Least squares analysis of MW- and IR-Data

In a second step we used IR-data combined with MW-transitions for the determination of molecular constants. The Fourier transform IR-data have been taken from the measurements at Oulu [8]. These data have been transformed to upper state combination differences for the ν_9, ν_6, and ν_5 fundamental levels. Most of the differences are from the ν_6 band which has ^{P}P- and ^{R}R-transitions extending far out in K. For ν_9 and ν_5 the ^{R}R- and ^{P}P-transitions, respectively, vanish rapidly with increasing K, thus limiting the upper state combination differences non-diagonal in K to low K-values, only.

For the analysis we used the same model for interactions in the ν_9, ν_6, and ν_5 levels as described in [8]. Basically this model takes into account first order *a*-Coriolis interactions within the tetrade ν_9, ν_6, ν_5, and ν_8 using Watsons *a*-reduced Hamiltonian. In addition, higher order perturbations between ν_6 and ν_9 and between ν_6 and ν_5 are included. The Hamiltonian matrix of the model and the definition of its parameters are given in Table 2 of [8].

The constants obtained from the fit are given in Tables 12–14. This fit was to 136 rotational data from the present work and 3198 upper state combination differences from the infrared measurements [8]. The data used in the fit were weighted according to the estimated uncertainty of the measurements. The uncertainty of our microwave measurements has been estimated to be 30 kHz, and of the Fourier transform data [8] 3×10^{-3} cm^{-1}. A weight of 10^6 was therefore used for the MW-data relative to the IR-data. In the fit we constrained the band center values and a few other of the constants to the values as obtained in [8]. In total we have determined 34 molecular parameters from this fit.

IV. Discussion

As with ground state constants (Table 8) the microwave data give poor estimates of the A and D_K constants because only *a*-type transitions can be observed in this very nearly prolate asymmetric top molecule [15]. For this reason the D_K (Δ_K) constant had to

Table 9. Molecular parameters of D_2C_2O in the $v_6=1$ state. * Fixed to the IR-MW value (Table 15). – The correlation coefficients which are near 1 in the *a*-reduced MW fit which are near 1 do not exceed the value of 0.8 in the IR-MW fit.

ROTATIONAL CONSTANTS

Watson's s-reduced			Watson's a-reduced		
A	131647(65)	MHz	A	131647(65)	MHz
B	9161.50(1)	MHz	B	9161.21(9)	MHz
C	8565.55(1)	MHz	C	8565.84(9)	MHz
D_J	2.84(3)	kHz	Δ_J	2.66(6)	kHz
D_{JK}	0.2810(4)	MHz	Δ_{JK}	0.2821(5)	MHz
D_K	3.3277	MHz *	Δ_K	3.3277	MHz *
d_1	-0.24(4)	kHz	δ_J	0.24(4)	kHz
d_2	0.09(3)	kHz	δ_K	-0.15(5)	MHz
H_{JK}	0.045(5)	kHz	Φ_{JK}	0.046(5)	kHz
H_{KJ}	-1.06(1)	kHz	Φ_{KJ}	-1.06(1)	kHz
		κ	-.9903		

CORRELATION MATRIX

	A	B	C	D_J	D_{JK}	d_1	d_2	H_{JK}	H_{KJ}
A	1.000								
B	-.016	1.000							
C	-.070	-.768	1.000						
D_J	.137	.282	.274	1.000					
D_{JK}	-.112	.206	.183	.425	1.000				
d_1	-.001	-.856	.853	-.006	-.015	1.000			
d_2	.740	-.025	-.032	.087	-.079	.009	1.000		
H_{JK}	.419	.130	.116	.677	.555	-.006	.309	1.000	
H_{KJ}	-.568	-.032	-.028	-.539	-.082	-.001	-.419	-.871	1.000

	A	B	C	Δ_J	Δ_{JK}	δ_J	δ_K	Φ_{JK}	Φ_{KJ}
A	1.000								
B	-.736	1.000							
C	.731	-.997	1.000						
Δ_J	-.587	.858	-.824	1.000					
Δ_{JK}	.396	-.571	.606	-.315	1.000				
δ_J	.001	.106	-.106	.012	.006	1.000			
δ_K	-.741	.994	-.994	.846	-.593	.010	1.000		
Φ_{JK}	.438	-.321	.350	.058	.664	.006	-.338	1.000	
Φ_{KJ}	-.594	.456	-.465	.129	-.365	.001	.463	-.873	1.000

STANDARD DEVIATION 90 kHz

Table 11. Molecular parameters of D_2C_2O in the ground state (recalculated from [6]).

ROTATIONAL CONSTANTS

Watson's s-reduced			Watson's a-reduced		
A	143730(51)	MHz	A	143730(51)	MHz
B	9123.98(1)	MHz	B	9124.41(8)	MHz
C	8570.99(1)	MHz	C	8570.56(8)	MHz
D_J	2.49(3)	kHz	Δ_J	2.71(5)	kHz
D_{JK}	0.3255(7)	MHz	Δ_{JK}	0.3242(7)	MHz
D_K	8.334	MHz *	Δ_K	8.334	MHz *
d_1	-0.21(4)	kHz	δ_J	0.21(4)	kHz
d_2	-0.11(2)	kHz	δ_K	0.21(4)	MHz
H_{JK}	2(3)	Hz	Φ_{JK}	2(3)	Hz
H_{KJ}	-0.31(2)	kHz	Φ_{KJ}	-0.31(2)	kHz
		κ	-.9918		

CORRELATION MATRIX

	A	B	C	D_J	D_{JK}	d_1	d_2	H_{JK}	H_{KJ}
A	1.000								
B	-.046	1.000							
C	-.074	-.730	1.000						
D_J	.141	.320	.292	1.000					
D_{JK}	-.379	.284	.214	.368	1.000				
d_1	.018	-.848	.853	-.015	-.032	1.000			
d_2	.640	-.051	-.027	.090	-.245	.024	1.000		
H_{JK}	.043	.262	.221	.696	.707	-.021	.026	1.000	
H_{KJ}	-.471	.189	.132	.063	.868	-.025	-.305	.320	1.00

	A	B	C	Δ_J	Δ_{JK}	δ_J	δ_K	Φ_{JK}	Φ_{KJ}
A	1.000								
B	-.636	1.000							
C	.628	-.996	1.000						
Δ_J	-.475	.834	-.792	1.000					
Δ_{JK}	-.170	-.056	.114	.158	1.000				
δ_J	-.018	.124	-.123	.029	.025	1.000			
δ_K	-.639	.993	-.993	.818	-.090	.024	1.000		
Φ_{JK}	.010	.057	-.001	.422	.730	.023	.025	1.000	
Φ_{KJ}	-.459	.301	-.266	.284	.795	.025	.282	.338	1.000

STANDARD DEVIATION 82 kHz

Table 10. Molecular parameters of D_2C_2O in the $v_9=1$ state. * Fixed to the IR-MW value (Table 15). – The correlation coefficients which are near 1 in the *a*-reduced MW fit which are near 1 do not exceed the value of 0.8 in the IR-MW fit.

Rotational constants			
A	141492(16)	MHz	
B	9120.833(3)	MHz	
C	8552.699(3)	MHz	
Centrifugal distortion constants			
D_J	2.49(1)	kHz	
D_{JK}	0.3230(3)	MHz	
D_K	4.3228	MHz	fixed
d_1	−0.22(1)	kHz	
d_2	−0.111(8)	kHz	
H_{JK}	3(1)	Hz	
H_{KJ}	−0.132(9)	kHz	
Standard deviation		28 kHz	

Table 12. Comparison of molecular parameters of D_2C_2O in the $v_5=1$ state. Data are given in cm^{-1}. * Fixed to the IR-MW value (Table 15).

	MW-Data	IR + MW-Data
A	4.79432(170)	4.74236(13)
$(B+C)/2$	0.29512017(12)	0.29512037(4)
$(B-C)/2$	0.0092370(3)	0.0092783(9)
$10^7 \cdot \Delta_J$	0.904(16)	0.971(5)
$10^4 \cdot \Delta_{JK}$	0.10811(23)	0.11309(7)
$10^4 \cdot \Delta_K$	2.78*	2.78
$10^8 \cdot \delta_J$	0.700(133)	0.741(25)
$10^5 \cdot \delta_K$	0.700(133)	0.99(4)
$10^{10} \cdot \Phi_{JK}$	0.667(1001)	
$10^7 \cdot \Phi_{KJ}$	−0.100(7)	−0.080(3)

be fixed to the values given in the IR-MW fit in order to get acceptable matrices of the correlation coefficients.

A comparison of the given fits for *s*- and *a*-reduction Hamiltonian in v_5, v_6, and v_9 is not possible because of the different definition of some distortion constants. Nevertheless it can be noted that the *a*-reduction parameters have a larger error and that more correlation coefficients approach unity.

It was already shown by Johns et al. [15] and Mallinson and Nemes [16] that the A constant differs considerable if one compares values obtained combining MW + IR measurements with values obtained from MW-spectra alone. This happens particularly for H_2CCO and HDCCO but not for D_2CCO, in the ground state, where the difference is only 0.00034 cm^{-1} outside the error limits (see Table 1 in [8]).

Table 13. Comparison of molecular parameters of D_2C_2O in the $v_6=1$ state. Data are given in cm^{-1}. * Fixed to the IR-MW value (Table 15).

	MW-Data	IR + MW-Data
A	4.85248(197)	4.651827(12)
$(B+C)/2$	0.29507914(19)	0.29507914(3)
$(B-C)/2$	0.0090056(5)	0.0090612(3)
$10^7 \cdot \Delta_J$	0.874(33)	0.8629(16)
$10^4 \cdot \Delta_{JK}$	0.1058(3)	0.0751(6)
$10^4 \cdot \Delta_K$	0.905*	0.905(17)
$10^8 \cdot \delta_J$	0.67(7)	0.710(5)
$10^5 \cdot \delta_K$	−0.63(30)	0.338(7)
$10^8 \cdot \Phi_{JK}$	0.781(13)	0.0018(3)
$10^7 \cdot \Phi_{KJ}$	−0.230(7)	−0.1004(20)

Table 14. Comparison of molecular parameters of D_2C_2O in the $v_9=1$ state. Data are given in cm^{-1}. * Fixed to the IR-MW value (Table 15).

	MW-Data	IR + MW-Data
A	4.39128(217)	4.77780(14)
$(B+C)/2$	0.29565537(19)	0.29565513(5)
$(B-C)/2$	0.0099297(5)	0.0100144(5)
$10^7 \cdot \Delta_J$	0.887(20)	0.972(6)
$10^4 \cdot \Delta_{JK}$	0.09410(17)	0.1144(6)
$10^4 \cdot \Delta_K$	1.11*	1.11(6)
$10^8 \cdot \delta_J$	0.80(13)	0.99(5)
$10^5 \cdot \delta_K$	−0.47(17)	0.72(3)
$10^8 \cdot \Phi_{JK}$	0.150(17)	0.0593(20)
$10^7 \cdot \Phi_{KJ}$	−0.3536(33)	−0.3217(18)

Table 15. Molecular parameters of D_2C_2O in the $v_5=1$, $v_6=1$, and $v_9=1$ states obtained from a simultaneous analysis of rotational transitions and upper states combination differences from the infrared spectrum[a].

	v_5	v_6	v_9
v_0	[541.19152][b]	[434.72348][b]	[371.55633][b]
A	4.74236(13)	4.651827(12)	4.77780(14)
$(B+C)/2$	0.29512037(4)	0.29507914(3)	0.29565513(5)
$(B-C)/2$	0.0092783(9)	0.0090612(3)	0.0100144(5)
$10^7 \cdot \Delta_J$	0.971(5)	0.8629(16)	0.972(6)
$10^4 \cdot \Delta_{JK}$	0.11309(7)	0.0751(6)	0.1144(6)
$10^3 \cdot \Delta_K$	[0.278][b]	0.0905(17)	0.111(6)
$10^{11} \cdot \Phi_J$	0.38(5)	[0.0]	[0.0]
$10^{10} \cdot \Phi_{JK}$	[0.0]	0.18(3)	5.93(20)
$10^8 \cdot \Phi_{KJ}$	−0.80(3)	−1.004(20)	−3.217(18)
$10^7 \cdot \Phi_K$	[−4.16][b]	−0.87(4)	[6.69][b]
$10^8 \cdot \delta_J$	0.741(25)	0.710(5)	0.99(5)
$10^5 \cdot \delta_K$	0.99(4)	0.338(7)	0.72(3)
$10^3 \cdot \eta^{bc}_{6,9}$		−0.1919(21)	
$10^4 \cdot \eta^{J}_{6,9}$		−0.435(6)	
$10^2 \cdot \eta^{K}_{6,9}$		−0.6322(14)	
$10^3 \cdot w_{5,6}$	0.747(4)		
$10^2 \cdot \eta^{K}_{5,9}$		[0.565][b]	

[a] All constants are given in cm^{-1}. Uncertainties quoted are standard deviations. The upper state combination differences are from [8].

[b] Constrained to the value obtained in [8].

The same does not seem to happen for our data. In fact a very large discrepancy is found for ν_9 (Table 14), where the difference in A is 0.38 cm^{-1}, more than 100 times the standard deviation, and for ν_6 (Table 13), where the difference is a little less but still 0.2 cm^{-1}. The best agreement is found for ν_5, where the difference is 0.05 cm^{-1}.

Why is there such a large disagreement in the excited states, but not in the ground state? If we compare both fitting procedures we see that the IR + MW-data have been fit to Coriolis interactions between ν_8, ν_9 (B_2) and ν_6, ν_5 (B_1). As was pointed out by Nemes there are first order a-type interactions between these levels as well as some second order interactions which are expressed by the constants η_{69}^{bc} and w_{56} (see Table 3 in [8]).

Since the position of the lines in the MW-spectrum could be explained with a normal centrifugal distortion analysis, we did not include any Coriolis interaction constants in the microwave data fit. Our MW-constants are therefore effective constants containing some contribution of this interaction.

The contribution to the A-rotational constants due to a-Coriolis interaction may be obtained as the difference between the A-constants obtained from the MW-fit and the A-constants obtained from the IR + MW-fit. For ν_5, ν_6, and ν_9 we obtain $\Delta A(\mathrm{Cor}) = 0.0520(17)\ cm^{-1}$, $0.2007(20)\ cm^{-1}$, and $-0.3865(22)\ cm^{-1}$, respectively, from Tables 12–15. Using the first order Coriolis interaction constants given in Table 3 in [8] the following Coriolis contributions may be predicted for ν_5, ν_6, and ν_9 from second order perturbation theory: $0.049\ cm^{-1}$, $0.159\ cm^{-1}$, and $-0.401\ cm^{-1}$. This shows that most of the observed Coriolis contributions to the A-rotational constants derive from a-Coriolis interactions within the tetrade ν_8, ν_5, ν_6, and ν_9.

The reason why we could not see any shift of lines from the K-levels where such shifts exist in the IR-spectra, can be explained if we look at Fig. 3 of [8].

We see there that the difference between two neighboring K-levels at $K=5$ in ν_9, for instance, is of the order of 40 cm^{-1}, while $(B+C)/2$ is about 0.3 cm^{-1}. So we have in the symmetric top limit a ladder of J levels for each K, spaced of multiples of 0.6 cm^{-1}. In the case of an interaction concerning the K-levels, the complete ladder will be shifted, giving practically no change in the a-type microwave spectrum, where only transitions between the J-levels inside a given K-level are possible. The way to see an effect would be to measure K-doublet transitions of high J-levels, as was done for CD_2O [17, 18].

Any attempt to adjust the MW-constants to the IR + MW-constants using a program which only takes into account the Coriolis coupling of two interacting vibrational states, e.g. ν_6 and ν_9, gave unacceptable results because the other simultaneous interactions were neglected. On the other hand, the standard deviation of the microwave transitions is of the same order of magnitude in the MW-fit and the IR + MW-fit, so we believe that the constants derived from the IR + MW-fit are more reliable.

Acknowledgements

We wish to thank the Deutsche Forschungsgemeinschaft and the Fonds der Chemie for research funds and grants. Furthermore we thank the members of the group in Kiel for discussions, the workshop of the Institut für Physikalische Chemie for technical assistance and Prof. Dr. M. Gerry for discussions and critical reading of the manuscript. Prof. Dr. M. Winnewisser and Dr. L. Nemes are thanked for given us their line frequencies.

[1] B. Bak, E. S. Knudsen, E. Madsen, and J. Rastrup-Andersen, Phys. Rev. **79,** 190 (1950).
[2] H. R. Johnson and M. W. P. Strandberg, Phys. Rev. **82,** 327a (1952).
[3] H. R. Johnson and M. W. P. Strandberg, J. Chem. Phys. **20,** 687 (1952).
[4] C. B. Moore and G. C. Pimentel, J. Chem. Phys. **38,** 2816 (1963).
[5] A. P. Cox, L. F. Thomas, and J. Sheridan, Spectrochim. Acta **15,** 542 (1959).
[6] L. Nemes and M. Winnewisser, Z. Naturforsch. **31a,** 272 (1976).
[7] L. Nemes and M. Winnewisser, private communication.
[8] F. Hegelund, J. Kauppinen, and F. Winther, Mol. Phys. **61,** 261 (1987).
[9] J. Kauppinen, Appl. Optics **14,** 1984 (1974), Acta Univ. Oulu A, **38** (1975).
[10] J. Kauppinen, Appl. Optics **18,** 1788 (1979).
[11] A. Savitzky and M. J. E. Golay, Anal. Chem. **36,** 1627 (1964).
[12] L. Nemes, J. Mol. Spec. **72,** 102 (1978).
[13] E. H. Putley, Appl. Optics **4,** 649 (1965).
[14] A. P. Cox and A. S. Esbitt, J. Chem. Phys. **38,** 1636 (1963).
[15] J. W. C. Johns, J. M. R. Stone, and G. Winnewisser, J. Mol. Spectrosc. **42,** 523 (1972).
[16] P. D. Mallinson and L. Nemes, J. Mol. Spectrosc. **59,** 470 (1976).
[17] M. Allegrini, J. W. C. Johns, and A. R. W. McKellar, J. Mol. Spectrosc. **67,** 476 (1977).
[18] D. Dangoisse, E. Willemot, and J. Bellet, J. Mol. Spectrosc. **71,** 414 (1978).